ChemPubSoc Europe

DOI: 10.1002/cssc.201600330

CHEMSUSCHEM Communications

Human Urine-Fueled Light-Driven NADH Regeneration for Redox Biocatalysis

Woo Seok Choi[+], Sahng Ha Lee[+], Jong Wan Ko, and Chan Beum Park*[a]

Human urine is considered as an alternative source of hydrogen and electricity owing to its abundance and high energy density. Here we show the utility of human urine as a chemical fuel for driving redox biocatalysis in a photoelectrochemical cell. $Ni(OH)_2$-modified α-Fe_2O_3 is selected as a photoanode for the oxidation of urea in human urine and black silicon (bSi) is used as a photocathode material for nicotinamide cofactor (NADH: hydrogenated nicotinamide adenine dinucleotide) regeneration. The electrons extracted from human urine are used for the regeneration of NADH, an essential hydride mediator that is required for numerous redox biocatalytic reactions. The catalytic reactions at both the photoanode and the photocathode were significantly enhanced by light energy that lowered the overpotential and generated high currents in the full cell system.

Solar energy has attracted significant attention owing to global demands for sustainable energy from alternative and renewable resources.[1–3] The synthesis of valuable chemicals through the solar degradation of organic wastes, such as human or animal urine, can benefit energy and environmental aspects.[4–6] Human urine contains a high amount of urea (~0.33 M), a useful hydrogen carrier owing to its stability, nontoxicity, and non-flammability,[7] which is widely used as a fertilizer in agriculture.[8] The conventional method for obtaining hydrogen from urea involves an energy-intensive process, such as thermal cracking of ammonia from urea decomposition,[9] while simultaneous production of energy (e.g., electricity, hydrogen) and degradation of urea/urine can be achieved by electrochemical,[10,11] photochemical,[12] and photoelectrochemical[13] reactions. Photoelectrochemical oxidation of urea is a cost-effective, safe, and sustainable approach to draw electrons from urea for solar fuel production by utilizing renewable sources like sunlight to reduce the energy required for electrochemical method.

On the other hand, biochemical approach for energy storage is an alternative way to realize artificial photosynthesis through coupling a redox enzymatic reaction with the light-driven regeneration of nicotinamide cofactor [NAD(P)H: hydrogenated nicotinamide adenine dinucleotide (phosphate)].[14,15] As a biological form of hydrogen carrier, NAD(P)H can be utilized by numerous and novel biocatalytic redox reactions that can produce value-added chemical products with high selectivity under environmentally benign conditions.[16] Thus, biocatalytic reduction chemistry has attracted considerable interests as a greener alternative to traditional chemical catalysis.[17] The capability of the redox biocatalyst depends on the supply of stoichiometric amount of redox equivalents, and intensive studies have focused on the issue over the past two decades.[16] Whereas the biochemical regeneration method has long been studied for the preparative use of biocatalytic chemistry, electrochemical (or photoelectrochemical) regeneration of NAD(P)H has been suggested as a cleaner and more energy efficient approach.[15]

In this paper, we report a human urine-fueled photoelectrochemical (PEC) cell platform for visible light-driven redox biocatalysis. As depicted in Figure 1, the biocatalytic PEC cell is configured with a dual semiconductor photoelectrode system consisting of a photoanode [$Ni(OH)_2$-modified α-Fe_2O_3 nanowires] and a photocathode (nanoporous black silicon, bSi) for the regeneration of a NADH. The photo-induced extraction of electrons from urea in human urine occurs on the photoanode, which is simultaneously coupled with the cathodic reaction for NADH regeneration and redox biocatalysis.

We used earth-abundant, non-toxic α-Fe_2O_3 as a photoanode material because it has good photochemical stability and a narrow bandgap ($E_g \approx 2.0$ eV) that is suitable for visible-light

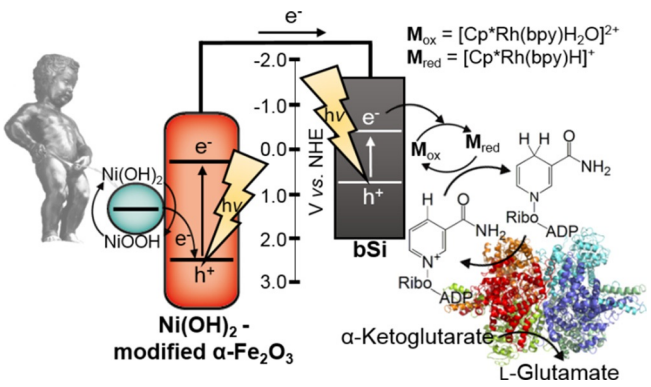

Figure 1. A human urine-fueled photoelectro-chemical cell for redox biocatalysis. When $Ni(OH)_2$-modified α-Fe_2O_3 is illuminated, incident photons excite the α-Fe_2O_3, generating electron and hole pairs. The holes are involved in the oxidation of $Ni(OH)_2$ to NiOOH, which is subsequently reduced to initial form by urea oxidation. The electrons from α-Fe_2O_3 drift to black silicon (bSi, photocathode) through an external circuit. The electrons are used to compensate for holes generated in bSi by photons, while excited electrons in the photocathode are used to reduce the nicotinamide cofactor for an enzymatic reaction through an electron mediator (M).

[a] W. S. Choi,[+] Dr. S. H. Lee,[+] J. W. Ko, Prof. Dr. C. B. Park
Department of Materials Science and Engineering
Korea Advanced Institute of Science and Technology (KAIST)
335 Science Road, Daejeon 305-701 (Republic of Korea)
E-mail: parkcb@kaist.ac.kr

[+] These authors contributed equally to this work.

Supporting Information and the ORCID identification number(s) for the author(s) of this article can be found under http://dx.doi.org/10.1002/cssc.201600330.

absorption.[18,19] We modified α-Fe_2O_3 nanowires with an $Ni(OH)_2$ catalyst to facilitate urea oxidation. Urea is oxidized in an alkaline solution by an $Ni(OH)_2$ catalyst according to the following mechanism:[20]

$$\text{C step}: \quad 6\,NiOOH_{(s)} + CO(NH_2)_{2(aq)} + H_2O_{(l)} \rightarrow 6\,Ni(OH)_{2(s)} + N_{2(g)} + CO_{2(g)} \quad (1)$$

$$\text{E step}: \quad 6\,Ni(OH)_{2(s)} + 6\,OH^- \rightarrow 6\,NiOOH_{(s)} + 6\,H_2O_{(l)} + 6\,e^- \quad (2)$$

Net anodic reaction:

$$CO(NH_2)_{2(aq)} + 6\,OH^- \rightarrow N_{2(g)} + 6\,H_2O_{(l)} + CO_{2(g)} + 6\,e^- \quad (3)$$

Electrochemical oxidation of urea undergoes an indirect oxidation mechanism that involves the reduction of NiOOH to $Ni(OH)_2$ (C step), followed by the regeneration of $Ni(OH)_2$ to NiOOH (E step). Visible-light absorption by α-Fe_2O_3 generates excited holes and electrons to more efficiently drive the E step. The separated holes oxidize the $Ni(OH)_2$ (i.e., Ni^{2+} oxidation state) catalyst on the surface of α-Fe_2O_3 to produce NiOOH (i.e., the Ni^{3+} oxidation state) in alkaline conditions. Then, urea is decomposed into CO_2 and N_2, along with the reduction of NiOOH into $Ni(OH)_2$. Consequently, the photo-excited electrons that are generated on the photoanode are transferred to the photocathode through an external circuit to run the following cascade of reactions:

$$bSi + h\nu + e^- \rightarrow bSi(e_{CB}{}^- + h_{VB}{}^+) + e^- \rightarrow bSi(e_{CB}) \quad (4)$$

$$M_{ox} + 2\,e^- + H^+ \rightarrow M_{red} \quad (5)$$

$$NAD^+ + M_{red} \rightarrow NADH + M_{ox} \quad (6)$$

$$\alpha\text{-ketoglutarate} + NH_4{}^+ + NADH \rightarrow \text{L-glutamate} + NAD^+ + H_2O \quad (7)$$

The bSi is a good photocathode material that can enhance photon absorption through low reflectance.[21] We used bSi as a counter electrode material for visible light-induced NADH generation. Upon light illumination, the excited holes in the bSi electrode ($h_{VB}{}^+$, VB: valence band) combine with the electrons that are transferred from the anode side and the excited electrons in the cathode ($e_{CB}{}^-$, CB: conduction band) reduce NAD^+ to NADH through an electron mediator, M {$[Cp^*Rh(bpy)(H_2O)]^{2+}$, M_{ox}: oxidized form, M_{red}: reduced form}. M acts as a hydride transfer reagent for the regeneration of enzymatically active 1,4-NADH with high activity, selectivity, and stability.[22] Finally, the reduced form of cofactor is applied to the enzymatic turnover. As a model redox enzyme, we utilized L-glutamate dehydrogenase (GDH) that can convert α-ketoglutarate to L-glutamate only in the presence of 1,4-NADH.

We synthesized α-Fe_2O_3 nanowire arrays with a hydrothermal method.[13] The synthesized α-Fe_2O_3 grew in the form of nanowires according to our scanning electron microscopic (SEM) images (Figure S1 in the Supporting Information), which exhibited a typical X-ray diffraction (XRD) pattern of α-Fe_2O_3 (Figure S2). The α-Fe_2O_3 nanowires had a band gap of approximately 2.14 eV according to the Tauc plot obtained from UV/Vis absorption spectra (Figure S3). We modified α-Fe_2O_3 nanowires with $Ni(OH)_2$ through a dip-coating method and confirmed the coexistence of the Ni species in the hybrid materials by energy dispersive X-ray spectroscopy (EDX) and X-ray photoelectron spectroscopy (XPS) (Figures S1 and S4). We observed urea oxidation on bare and $Ni(OH)_2$-modified α-Fe_2O_3 nanowires by using linear sweep voltammetry (LSV). As shown in Figure S6, $Ni(OH)_2$-modified α-Fe_2O_3 exhibited an oxidation peak at around 0.6 V (vs. Hg/HgO) in an alkaline solution (1 M NaOH), which corresponds to the oxidation of $Ni(OH)_2$ (E step) according to the literature.[20,23] The intensity of the oxidation peak increased upon the addition of 10 mM urea owing to the electrocatalytic oxidation of urea. The oxidation reaction involves NiOOH reduction to $Ni(OH)_2$ (C step). In contrast, bare α-Fe_2O_3 showed an anodic current that occurred at 0.75 V (vs. Hg/HgO) without any significant change in the presence of urea (Figure S7). The result indicates that the electrochemical oxidation of urea can be carried out efficiently by the Ni catalyst [i.e., $Ni(OH)_2$], whereas bare α-Fe_2O_3 lacks catalytic activity on urea oxidation.

Electrochemical oxidation of urea was significantly enhanced by visible-light illumination of $Ni(OH)_2$-modified α-Fe_2O_3. Figure 2a shows visible light-enhanced catalytic activity of $Ni(OH)_2$ for the oxidation of urea. In a 10 mM urea electrolyte, the onset potential (V_{onset}) for Ni catalyst oxidation showed a large cathodic shift from 0.42 to −0.3 V by light illumination, which indicates that urea oxidation can be improved by photon absorption. In the case of bare α-Fe_2O_3, the intensity of photocurrent generation was negligible in comparison to the current generation from an $Ni(OH)_2$-modified α-Fe_2O_3 electrode (Figure S7), indicating that the bare α-Fe_2O_3 itself is not catalytically active toward urea oxidation. The coupling of the electrocatalyst [$Ni(OH)_2$] with the photoanode (α-Fe_2O_3) resulted in a significant decrease in the potential required for the electrooxidation of urea.[10,11] The increase of urea concentration induced an increase of anodic current at around 0 V (vs. Hg/HgO; Figure S8). We confirmed the above catalytic behavior of $Ni(OH)_2$-modified α-Fe_2O_3 in human urine, as shown in Figure S9.

We investigated the role of bSi as a photocathode material that enhances photoelectrochemical reactions. Fabricated by a metal-assisted chemical etching method,[24] bSi has a highly porous nanostructured surface with a reflectance of less than 10% over the entire visible-light range (300–800 nm, Figure S5). Figure 2b shows the current–potential curves in a two-electrode system configured with $Ni(OH)_2$-modified α-Fe_2O_3 as a working electrode and bSi as a counter electrode. The onset potential for urea oxidation cathodically shifted from 0.8 to 0.0 V upon illumination on $Ni(OH)_2$-modified α-Fe_2O_3, and the onset potential further shifted from 0.0 to −0.1 V upon illumination of the bSi photocathode. This result indicates that the PEC reaction driven by an $Ni(OH)_2$-modified α-Fe_2O_3 photoanode can be further enhanced by a bSi photocathode. In contrast to the bSi photocathode, no photoresponse was observed when bare platinum was used as a counter electrode (Figure S10). A chronopotentiometric measurement under

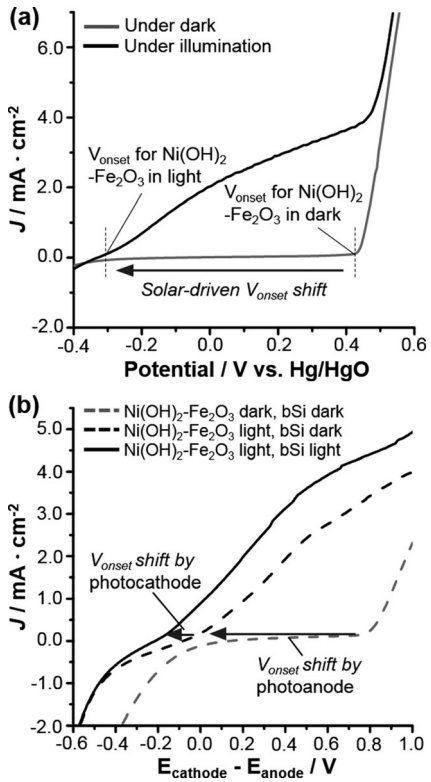

Figure 2. Linear sweep voltammograms (LSVs) of $Ni(OH)_2$-modified α-Fe_2O_3 (50 mV s^{-1}) were obtained with (a) a three-electrode and (b) a two-electrode system under dark and illuminated conditions. $Ni(OH)_2$-modified α-Fe_2O_3 was immersed in a 1 M NaOH aqueous solution with 10 mM of urea. In the three-electrode system, Hg/HgO was used as a reference electrode and a platinum wire was used as a counter electrode. In the two-electrode system, the counter electrode was bSi immersed in a 50 mM phosphate buffer (pH 7.5).

a constant current of -10 μA also confirmed the contribution of each electrode on photovoltage generation (Figure S11).

We conducted a solar-assisted regeneration of NADH from NAD^+ in a photoelectrochemical cell operating with a three-electrode system that consisted of an $Ni(OH)_2$-modified α-Fe_2O_3 photoanode (working electrode), a bSi photocathode (counter electrode), and an Hg/HgO reference electrode. NADH did not form in the dark condition at a static applied potential of 0 V (vs. Hg/HgO; Figure 3a, Figure S12). When we illuminated the PEC cell containing human urine (or 0.33 M urea), we observed NADH generation at a rate of 0.34 mM h^{-1}. However, with light only illuminating the $Ni(OH)_2$-modified α-Fe_2O_3 photoanode side, the rate of NADH regeneration was reduced to 0.17 mM h^{-1} (Figure S12). This result confirms the role of the bSi photocathode in improving the cathodic reaction upon light absorption. We speculate that the photoexcited charge carriers in bSi are extracted into the electrolyte by a space-charge-induced electric field at the junction, where they can drive a redox reaction in a kinetically favorable manner by reducing the required overpotential. It is deduced that the redox reaction (i.e., NAD^+ reduction) can be boosted by either enhanced photocurrent generation or reduced overpotential. As stated in the literature,[29] the silicon photocathode could drive the cathodic reaction efficiently by lowering the potential for NADH regeneration. Moreover, the anode-driven PEC platform reduced the required energy from external sources. Note that, unlike the result shown in Figure 2b, the photocurrent measured from the photoanode was not affected by the function of the photocathode in the three-electrode configuration (Figure S13). In a two-electrode system, the working electrode is referenced to the counter electrode that exhibits dynamic potential by photoexcitation. In the three-electrode system, the signal from the working electrode (i.e., the photoanode) is referenced to a static reference electrode (Hg/HgO), which can fix the complicated effects from the chemical potential and overcome the distance between the two functional electrodes.[25]

Because human urine is the main source of electrons required for the entire PEC reaction, we investigated NADH regeneration according to varied human urine concentrations by dilution with a 1 M NaOH aqueous solution (Figure 3b). In the absence of human urine, no NADH generation was observed in the biocatalytic PEC cell. As the concentration of human urine increased from 1 to 5 vol%, the NADH generation rate increased gradually from 0.008 to 0.28 mM h^{-1}. The reaction rate was further saturated at around 0.35 mM h^{-1} with 10 vol%

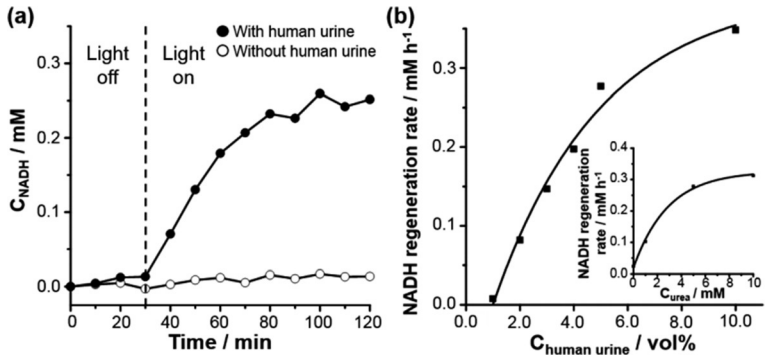

Figure 3. (a) Photoelectrochemical NADH regeneration using human urine. (b) The rate of NADH regeneration on varied human urine concentrations diluted with a 1 M aqueous NaOH solution. (Inset) NADH productivity under controlled urea concentrations (0, 1, 5, and 10 mM) in a 1 M NaOH solution. All reactions were conducted under visible light ($\lambda > 420$ nm) at 0 V vs. Hg/HgO. In (a), light in the anode [$Ni(OH)_2$-modified α-Fe_2O_3] side was turned on after 30 min of incubation under the dark, while the cathode (bSi) side was illuminated during the entire reaction time. In (b), all reactions were conducted under light illumination on both the anode and cathode electrodes.

human urine. Experiments with urea electrolytes also showed a similar tendency of productivity saturation at higher urea concentration (inset of Figure 3b). The photocurrent generation from $Ni(OH)_2$-modified α-Fe_2O_3 increased according to human urine concentration, which was also saturated at 0.4 mA with the human urine concentration at over 10 vol% (Figure S14). The similar early saturation behaviors from human urine and urea experiments indicate that the urea in human urine works as a source of electrons to regenerate $Ni(OH)_2$ from NiOOH. Note that the average concentration of urea in human urine is around 0.33 M,[10] which is enough to generate a current for NADH regeneration.

We further applied the human urine-fueled PEC platform to the enzymatic conversion of α-ketoglutarate to L-glutamate using NADH-dependent L-glutamate dehydrogenase. Figure 4a shows the concentration of synthesized L-glutamate in the biocatalytic reaction carried out under different illumination condition with an applied potential of 0.0 V (vs. Hg/HgO). When both electrodes were illuminated, the human urine-fueled, light-driven biocatalytic turnover resulted in a yield of 13.2% in 2 h through the regeneration of NADH. In the absence of light on the cathode side, the enzymatic conversion was significantly reduced to 4.8%. We observed that a higher level of

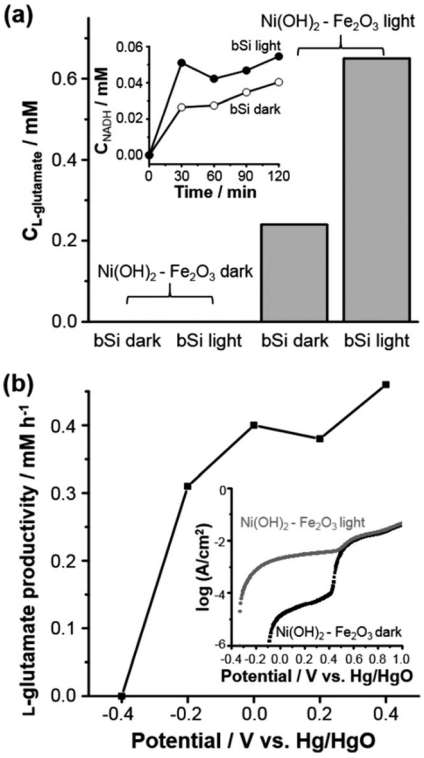

Figure 4. (a) Photobiocatalytic conversion of α-ketoglutarate to L-glutamate for 2 h under dark and light conditions with $Ni(OH)_2$-modified α-Fe_2O_3 and bSi photoelectrodes. (Inset) The concentration of regenerated NADH during enzymatic reaction under the condition in which $Ni(OH)_2$-modified α-Fe_2O_3 was illuminated. (b) L-Glutamate productivity under various external potentials (−0.4, −0.2, 0.0, 0.2, and 0.4 V) on a working electrode with illumination on both $Ni(OH)_2$-modified α-Fe_2O_3 and bSi. (Inset) The Tafel plot of $Ni(OH)_2$-modified α-Fe_2O_3 under dark and light conditions in a 1 M NaOH aqueous solution with 0.33 M urea.

NADH concentration was maintained when the bSi was illuminated during the biocatalytic reaction (inset of Figure 4a). Consistent with the result shown in Figure S12, this result suggests that the cathodic reaction can be boosted by the light energy. There was no conversion when the anode side was not illuminated during the reaction, regardless of the presence of light on the cathode side. Since the oxidation of urea requires a higher potential (i.e., around 0.5 V) in the absence of light as previously described in Figure 2a, photoexcitation of only the cathode is not sufficient to drive the biocatalytic reaction. Our result shows that the overall solar-powered reaction is driven by the photoanode at low bias potentials.

We investigated the effect of applied potential on the light-driven biocatalytic reaction by varying the applied potential from −0.4 to 0.4 V (Figure 4b). While there was no production of L-glutamate at the reaction potential of −0.4 V, the production rate increased to 0.31, 0.4, 0.38, and 0.46 mM h^{-1} under −0.2, 0.0, 0.2, and 0.4 V, respectively. The drastic difference that was observed between −0.4 and −0.2 V is attributed to the presence of the onset reaction potential. According to our Tafel analysis, the onset reaction potential was observed at approximately −0.32 V for $Ni(OH)_2$-modified α-Fe_2O_3 under light illumination (inset of Figure 4b). The Tafel plot obtained from a urea oxidation reaction under dark and light conditions clearly indicates that the shift in catalytic onset potential was driven by the photovoltaic effect of α-Fe_2O_3. In particular, the onset of linearity (E_{cat}), which corresponds to the energy required for urea oxidation,[26] showed a large cathodic shift in potential (740 mV) relative to that in dark conditions, thus indicating the superior catalytic activity of $Ni(OH)_2$-modified α-Fe_2O_3 for urea oxidation under visible light. We also confirmed the effect of onset potential on urea oxidation rate. There was no oxidation of urea observed at the working potential of −0.4 V, which is below the point of anodic photocurrent generation (Figure S15). Consistent with the enzymatic conversion over applied potentials, a gradual increase in the urea oxidation rate was also observed with increasing potential from −0.4 to 0.4 V.

In summary, we demonstrated that human urine is an attractive electron source for solar cofactor regeneration and redox biocatalysis. Visible light-driven oxidation of human urine was achieved by using $Ni(OH)_2$-modified α-Fe_2O_3 as a photoanode material. The accumulation of oxidation product in the biocatalytic reaction medium could be avoided by the separation of reduction and oxidation reactions, which makes our approach cleaner compared to the conventional photochemical methods carried out in a one-pot reactor. Driven by the light-induced oxidation of urea, the overall photoelectrochemical reactions could be carried out at near-zero potential, which is much lower than conventional electrochemical approaches.[22,29] The illumination on the photocathode made from black silicon (bSi) further enhanced cofactor regeneration rate, showing that light energy accelerates both cofactor regeneration and urea oxidation. Thousands of NADH-dependent enzymes are available in nature and the human urine-fueled biocatalytic PEC cell platform can be applied to virtually any NADH-dependent redox enzyme. The present study hints at an alternative solu-

tion to organic waste treatment by coupling it with enzymatic catalysis.

Experimental Section

Materials: Human urine was obtained from a healthy 26-year-old man. Urea, sodium hydroxide, iron(III) chloride hexahydrate, sodium nitrate, nickel(II) nitrate hexahydrate, hydrogen fluoride, silver nitrate, hydrogen peroxide, nitric acid, β-nicotinamide adenine dinucleotide (NAD^+), GDH from bovine liver, α-ketoglutarate, and ammonium sulfate were purchased from Sigma–Aldrich (USA). A boron-doped silicon wafer (1–10 Ω cm) was purchased from Tasco Co (Korea). $Cp^*Rh(bpy)(H_2O)^{2+}$ was synthesized according to the literature.[27]

Synthesis of α-Fe_2O_3 nanowire film: We synthesized α-Fe_2O_3 nanowire films by using a hydrothermal method.[13] After sequentially washing an FTO substrate in acetone, ethanol, and 2-propanol for 15 min each, we put the substrate in a solution of 0.15 M iron(III) chloride and 1 M sodium nitrate and incubated it in an autoclave. The autoclave was heated to 95 °C and cooled to room temperature after 4 h. Then, the substrate was washed with deionized water and heated to 600 °C for 8 h to improve the photoelectrochemical performance of the α-Fe_2O_3 film.[28]

$Ni(OH)_2$ deposition on α-Fe_2O_3 film: We deposited $Ni(OH)_2$ on α-Fe_2O_3 film according to the literature.[13] First, we dipped the α-Fe_2O_3 film in a 0.1 M $Ni(NO_3)_2$ solution for 10 s and dried it under an N_2 atmosphere. Then, the electrode was dipped into 1 M NaOH solution for another 10 s and dried with N_2 gas. The dip-coating cycle was repeated three times for the deposition of $Ni(OH)_2$.

Synthesis of black silicon: bSi was prepared by a metal-assisted etching method.[24] First, a silicon wafer was cut to a size of 10×30 mm and cleaned by immersing the wafer in acetone, ethanol, and 2-propanol, respectively (for 5 min each). To remove any organic impurities on the surface, we put the wafer in a piranha solution for 10 min. The cleaned wafer was washed with deionized water several times and immersed for 90 s in a 0.5 wt% HF solution containing 1 mM $AgNO_3$. Then, the wafer was dipped in an aqueous solution with a volume of 12.5% HF and 3% H_2O_2 for 40 s, transferred to an aqueous solution with a volume of 50% HNO_3 for a 13 min incubation, followed by rinsing with deionized water for 3 min and treating with 5% HF solution for 90 s. To make a bSi electrode, the etched wafer was cut into a 10×10 mm piece and connected to a copper wire with silver paste. The entire area, except for the reaction surface, was sealed with an epoxy resin.

Characterization: The morphologies of α-Fe_2O_3 and bSi were observed by using an S-4800 field emission SEM (Hitachi High-Technologies Co., Japan) at an electron acceleration voltage of 10 kV. EDX spectra were obtained by using XL 30 SFEG with EDAX (Philips, US) at an electron acceleration voltage of 20 kV. XRD measurements were conducted by using a RIGAKU Ultima IV X-ray diffractometer (Rigaku Co., Japan) with a scan rate of 4° min^{-1}, scan range of 20°–70°, and a CuK_α radiation wavelength of 1.5418 Å. We analyzed the surface composition of α-Fe_2O_3 and $Ni(OH)_2$-modifed α-Fe_2O_3 by using XPS with a K-alpha photoelectron spectrometer (Thermo VG Scientific, UK). All of the electrochemical measurements were performed by using a WMPG1000 potentiostat (WonATech, Korea). In a three-electrode system, Hg/HgO in a 1 M NaOH (0.140 V vs. standard hydrogen electrode) was used as a reference electrode and a platinum wire was used as a counter electrode in a 1 M NaOH solution under a 450-W Xe lamp illumination with a 420 nm cut-off filter. In a two-electrode system, bSi was used as a counter electrode, in which the working electrode compartment and the counter electrode compartment were connected by a salt bridge. UV/Vis absorption spectra were obtained by using a V650 spectrophotometer (JASCO Inc., Japan).

Cofactor regeneration and enzymatic synthesis of L-glutamate: NADH regeneration was conducted in the counter electrode compartment of a three-electrode system. $Ni(OH)_2$-modified α-Fe_2O_3 and bSi were used as a working electrode and a counter electrode, respectively, and both compartments were connected by a salt bridge. The working electrode compartment contained human urine or 0.33 M urea in a 1 M NaOH solution and the counter electrode compartment contained 1 mM NAD^+ and 250 μM M in a phosphate buffer (50 mM, pH 7.5). During photoelectrochemical NADH regeneration, we measured the change in NADH concentration according to the change of absorption intensity at 340 nm. Enzyme reactions were performed by using a phosphate buffer solution (50 mM, pH 7.5) that contained 40 U GDH, 1 mM NAD^+, 250 μM M, 5 mM α-ketoglutarate, and 0.1 M $(NH_4)_2SO_4$. We measured the L-glutamate concentration by using a 1260 Infinity liquid chromatography system (Agilent Technologies, US). The reaction samples were eluted by a phosphoric acid solution (0.05 wt%) at a flow rate of 1.0 mL min^{-1} and detected at 214 nm.

Measurement of urea concentration: We analyzed the change of urea concentration using a K-URAMR test kit (Megazyme International Ireland Ltd., Wicklow, Ireland). All tests were performed according to the procedure described in the manufacturer's instruction.

Acknowledgements

This study was supported by the National Research Foundation via the Creative Research Initiative Center (Grant number: NRF-2015R1A3A2066191), Republic of Korea.

Keywords: biocatalysis · human urine · NADH regeneration · photoelectrochemical cell · solar energy

[1] N. Armaroli, V. Balzani, *Angew. Chem. Int. Ed.* **2007**, *46*, 52–66; *Angew. Chem.* **2007**, *119*, 52–67.
[2] M. Grätzel, *Nature* **2001**, *414*, 338–344.
[3] M. G. Walter, E. L. Warren, J. R. McKone, S. W. Boettcher, Q. Mi, E. A. Santori, N. S. Lewis, *Chem. Rev.* **2010**, *110*, 6446–6473.
[4] P. Lianos, *J. Hazard. Mater.* **2011**, *185*, 575–590.
[5] R. L. King, G. G. Botte, *J. Power Sources* **2011**, *196*, 2773–2778.
[6] M. Antoniadou, P. Lianos, *Photochem. Photobiol. Sci.* **2011**, *10*, 431–435.
[7] A. N. Rollinson, J. Jones, V. Dupont, M. V. Twigg, *Energy Environ. Sci.* **2011**, *4*, 1216–1224.
[8] R. Lan, S. Tao, J. T. S. Irvine, *Energy Environ. Sci.* **2010**, *3*, 438–441.
[9] S. F. Yin, B. Q. Xu, X. P. Zhou, C. T. Au, *Appl. Catal. A* **2004**, *277*, 1–9.
[10] W. Yan, D. Wang, G. G. Botte, *Appl. Catal. B* **2012**, *127*, 221–226.
[11] W. Yan, D. Wang, G. G. Botte, *Electrochim. Acta* **2012**, *61*, 25–30.
[12] J. Kim, D. Monllor-Satoca, W. Choi, *Energy Environ. Sci.* **2012**, *5*, 7647–7656.
[13] G. Wang, Y. Ling, X. Lu, H. Wang, F. Qian, Y. Tong, Y. Li, *Energy Environ. Sci.* **2012**, *5*, 8215–8219.
[14] R. Ruppert, E. Steckhan, *J. Chem. Soc. Perkin Trans. 2* **1989**, 811–814.
[15] S. H. Lee, J. H. Kim, C. B. Park, *Chem. Eur. J.* **2013**, *19*, 4392–4406.
[16] a) A. Schmid, J. S. Dordick, B. Hauer, A. Kiener, M. Wubbolts, B. Witholt, *Nature* **2001**, *409*, 258–268; b) W. A. van der Donk, H. Zhao, *Curr. Opin. Biotechnol.* **2003**, *14*, 421–426.

[17] F. Hollmann, I. W. C. E. Arends, D. Holtmann, *Green Chem.* **2011**, *13*, 2285 – 2314.
[18] K. Sivula, F. Le Formal, M. Grätzel, *ChemSusChem* **2011**, *4*, 432 – 449.
[19] Y. Lin, G. Yuan, S. Sheehan, S. Zhou, D. Wang, *Energy Environ. Sci.* **2011**, *4*, 4862 – 4869.
[20] V. Vedharathinam, G. G. Botte, *Electrochim. Acta* **2012**, *81*, 292 – 300.
[21] J. Oh, T. G. Deutsch, H.-C. Yuan, H. M. Branz, *Energy Environ. Sci.* **2011**, *4*, 1690 – 1694.
[22] F. Hollmann, I. W. C. E. Arends, K. Buehler, *ChemCatChem* **2010**, *2*, 762 – 782.
[23] B. K. Boggs, R. L. King, G. G. Botte, *Chem. Commun.* **2009**, 4859 – 4861.
[24] J. Oh, H.-C. Yuan, H. M. Branz, *Nat. Nanotechnol.* **2012**, *7*, 743 – 748.
[25] J. Song, H. Lee, Y. Wang, C. Wan, *J. Power Sources* **2002**, *111*, 255 – 267.
[26] R. D. Smith, M. S. Prévot, R. D. Fagan, Z. Zhang, P. A. Sedach, M. K. J. Siu, S. Trudel, C. P. Berlinguette, *Science* **2013**, *340*, 60 – 63.
[27] H.-K. Song, S. H. Lee, K. Won, J. H. Park, J. K. Kim, H. Lee, S.-J. Moon, D. K. Kim, C. B. Park, *Angew. Chem. Int. Ed.* **2008**, *47*, 1749 – 1752; *Angew. Chem.* **2008**, *120*, 1773 – 1776.
[28] R. Morrish, M. Rahman, J. M. D. MacElroy, C. A. Wolden, *ChemSusChem* **2011**, *4*, 474 – 479.
[29] S. H. Lee, G. Ryu, J. H. Kim, C. B. Park, *ChemSusChem* **2014**, *7*, 3007 – 3011.

Received: March 10, 2016
Published online on May 20, 2016